27th ABCM International Congress of Mechanical Engineering
December 04-08, 2023, Florianópolis-SC, Brazil

COB-2023-0540
EXPERIMENTAL INVESTIGATION OF HYDRATE FORMATION IN CRUDE OIL AND HIGH SALINITY BRINES

Luiz Fernando Santos de Vasconcelos
Celina Kakitani
Moisés Alves Marcelino Neto
Rigoberto Eleazar Melgarejo Morales
Multiphase Flow Research Center – NUEM, Graduate Program in Mechanical and Materials Engineering – PPGEM, Federal University of Technology of Parana, Brazil
luizvasconcelos@alunos.utfpr.edu.br
ckakitani@gmail.com
mneto@utfpr.edu.br
rmorales@utfpr.edu.br

Amadeu K Sum
Phases to Flow Lab., Chemical and Biological Engineering Department, Colorado School of Mines, USA.
asum@mines.edu

Abstract. *In oil and gas production, forming hydrate plugs can lead to pipeline blockages, causing economic losses and safety issues. Extended shutdowns during oil and gas production can increase the potential risk of hydrate blockage when production is restarted. This work aims to characterize experimentally the process of hydrate formation in systems with high salt concentrations, with or without the addition of inhibitors and/or antiagglomerants. Also, to investigate the effect of high salinity brine on the flowability of hydrate formed by evaluating formation and transport under multiphase conditions, agglomeration, and bedding deposition in a rock-flow cell. Pressure, temperature, image data, and the estimated amount of hydrate formed were obtained. All experiments were conducted under constant pressure (60 bar and 80bar),in a three phase system, water and additives as aqueous phase, synthetic natural gas as gas phase and crude oil as oil phase). The hydrate formation were evaluated under different conditions: water cuts (10-50%) , liquid loading (30-50%), subcooling (5-15°C) and salt concentration (up to 16 wt%). In uninhibited systems, it was observed that the bedding profile is favored for higher water cuts, and for lower water cuts, the dispersed/wall deposition profile was obtained. The dispersed morphological profile was favored in scenarios where the salt concentration increased.*

Keywords: *hydrates, high-salinity, Crude oil, rock-flow cell*

1. INTRODUCTION

The risk of hydrate formation and the flow assurance must be evaluated under the study of several variables and their influence on each other cross effect. Factors such as subcooling, presence of inhibitors, water cut, gas/oil ratio, etc., uniquely impact the morphology/hydrate formation, which, when analyzed together, can add adverse influences or even be contrary to their effect.

After their formation and their possible agglomeration, a new non-flowing solid phase is created, and in gas and oil industries they can trigger blockages (Figure 1) in pipelines, causing damage and preventing normal operations. It is a flow assurance problem, where their occurrences can have high economic costs. The characterization of the hydrate formation and transportability is of significant importance.

Figure 1 -Hydrate plug being removed from a pipeline in a Petrobras installation.
Source: ONGC (2020)

The subcooling of a system is often studied when discussing gas hydrates kinetics. Defined as the difference between hydrate stability temperature and the actual operating temperature at the same pressure, considered a driving force, it can directly impact the morphological profile of the hydrates. When this temperature variation is high enough, a rapid formation can be favored, trapping the forming available water inside the structure and reducing further agglomeration (Mali et al., 2018).

There is no convention regarding a high/great subcooling interval. Mali et al. (2018) analyzed a specific subcooling interval. However, tests were conducted at six different pressures of 1.72, 2.76, 6.21, 6.89, 10.34, and 17.24 MPa with subcoolings from 3.2 K to 8.0 K. The results revealed that the scatter in induction time is higher at lower subcooling levels than at higher subcooling levels. The mean values of induction time reduce as the subcooling increases due to the greater thermodynamic driving force to form the hydrates. The authors also state that induction time is logarithmically related to natural gas and distilled water system subcooling (Mali et al., 2018) . According to Umuteme et al. (2022), the formation of hydrates is instantaneous at the right subcooling temperature. Additionally, hydrate deposition velocity is assumed to be constant for a fully developed turbulent flow in the pipeline. (Umuteme et al., 2022)

Hydrate deposition can lead to forming a solid plug that obstructs the flow in a pipeline. The plugging risk depends on several factors, including the hydrate deposition rate, the flow pattern, phase disposition, the subcooling temperature, and the pipeline geometry. In liquid-dominated pipelines, the liquid phase is continuous, and the gas phase is dispersed. In contrast, in gas-dominated pipelines, the gas phase is continuous, and the liquid phase is dispersed. The difference in the flow pattern and phase distribution affects the hydrate formation and deposition rate, as well as the plugging flow time and pressure drop. Therefore, it is essential to consider the dominant phase in the pipeline when observing hydrate deposition and plugging.

Higher hydrate formation risks are possible in gas-dominant pipelines because of the lower volume fraction of liquid water. The formation and agglomeration of hydrates are characterized by phase change and can be measured by the gas flow rate in the fluid domain. Experimental results suggest an increase in gas flow rate during hydrate formation because of the increased gas consumption rate. Also, the gas flow rate is relatively stable during agglomeration and decreases during hydrates deposition because of a reduction in pipe hydraulic diameter (Zerpa et al., 2011). In systems with higher liquid loads, it is observed to have higher mixture velocities due to more significant shear, favoring the transportability of hydrates once formed. Another aspect that implies that smaller loads of liquids tend to present a greater risk is directly associated with a more extensive layer of gas, consequently more gas available for forming hydrates.

According to Inemugha and Ajienka (2020), the water cut affects the cool-down time during an unplanned shutdown scenario. They analyzed the cool-down time for different water cuts representing the mid-life and late life of the field. For the 50% water cut representing the mid-life of the field, it took around 4 to 5 hours for the fluid to cool down to its ambient temperature from a shut-in temperature and pressure(Inemugha et al., 2020).

Zhou et al. (2018) investigated the formation and flow characteristics in systems with high water cuts. They observed that as the water cut increases, the friction coefficient increases, and the flow time decreases in the flow of the slurry. That means that high water cuts, hydrate nucleation, and mass production mainly occur at the gas-water interface, and due to the deposition and aggregation of the hydrates, the change in moving bed to fixed bed will result in the plug. For medium water cuts conditions, hydrate nucleation and formation mainly occur at the oil-water interface, and the accumulation of hydrate particles formed by water-in-oil is less. Eventually, it will get plugged due to the increase in viscosity and the accumulation of the deposits formed. Eventually, getting plugged due to the increase in viscosity and the accumulation of the deposits(Zhou et al., 2018).

Another feature that impacts the morphological arrangement of hydrates and inhibition, whether thermodynamic or kinetic, is the presence of inhibitors. Sodium chloride and anti-caking agents can help in the non-formation of hydrates or the controlled formation, that is, without caking. Liu et al. (2022) conducted experimental trials in water-in-oil emulsions with various salinities in rich aqueous phase systems by using a high-pressure rheometer. The results suggested that the increase in the salt concentration could slow the hydrate formation rate and reduce the water conversion rate. The hydrate slurry viscosity was also significantly reduced, and its stability was greatly improved (Liu et al., 2022).

Salts act as thermodynamic inhibitors, not allowing the formation of gas hydrates, however antiagglomerants agents act as kinetic inhibitors in the phenomenon of hydrate formation, inhibiting the possibility of agglomeration of these formed hydrates. In other words, hydrates can form, but flow assurance is guaranteed. There is no consensus regarding cross-setting when salt and AA are present. There is a gap regarding the potentiation or deactivation effect of the interfacial tension reduction effect due to the use of anti-caking agents. Ren et al. (2020) observed that under low-concentration NaCl conditions, anionic surfactants were very effective in accelerating methane hydrate formation and the final conversion of water to methane hydrate. Furthermore, he also finds that the high salt concentration can seriously damage the internal hydrogen bond network of the solution and consequently inhibit hydrate nucleation and nucleate growth (Ren et al., 2020).

There is no consensus between the use of higher or lower salt concentrations and/or the use of kinetic inhibitors. Among these, the set of these numerous risk variables must be analyzed and a detailed review of this impact on the formation of hydrates must be raised so that parameters and operating conditions are performed in a safe region.

2. METHODOLOGY

A rock-flow cell (Figure 2) was used to observe the flow development and the hydrate formation. The cell had an internal cylindrical shape, a total volume of 1000 ml and was designed to operate up to 100 bar.

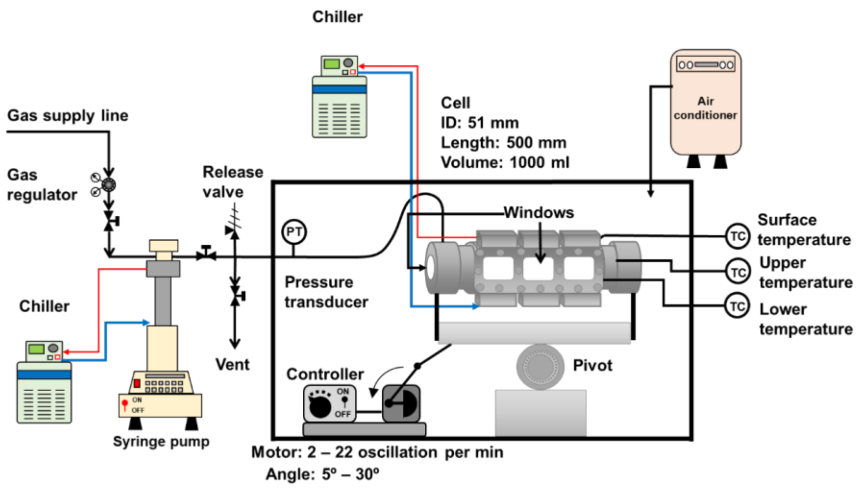

Figure 2 -Schematic of the rock-flow cell setup.

The rock-flow cell oscillations promoted the mixing of the fluids by gravity and fluid density differences. The cell can be operated with different inclinations (up to 20º) and oscillation rates (5 to 30 rpm). All experiments were performed with a pipe inclination of 20º and oscillation rates of 16 rpm. The cell had eight transparent windows made of polycarbonate – three windows at the front and three at the rear, and one round window on each side of the cell. The interior sides of the windows were milled in such a way that their profiles matched the curvature of the pipe. Four webcams captured the images from the front and left side views. The remaining windows were used to provide illumination. In addition to the video images, pressure and temperature data were gathered throughout the experiment.

The cell temperature was controlled by separate cooling chambers placed at the top and bottom surfaces to control the inner wall temperatures independently. The pressure sensor was installed in the gas line and the temperature sensors were installed in different sections of the rock-flow cell to measure the temperature of the upper and lower surfaces. The syringe pump supplied the gas used in the experiment and was used to pressurize the rock-flow cell and to keep the pressure (isobaric conditions) stable throughout the experiment. The syringe pump was also used to monitor variations in gas volume as the system was maintained at a constant pressure. A chiller was connected to the syringe pump to minimize any temperature effects on the volume measurements due to oscillations in the ambient temperature.

The impact of different parameters, such as liquid loading (30-60 vol%), water cut (0-50 %), and salt concentration (0, 3, 16 wt%) on the flow pattern and hydrate formation were investigated. All experiments used bacalhau crude oil as the oil phase and distilled water as the aqueous phase, with and without salt mixture addition (NaCl and $CaCl_2$). A gas mixture containing methane/propane and synthetic natural gas were used as the gas phase in the experiments. The gas compositions were shown in Table 1. All experiments were performed under isobaric conditions, at 60 bar and an initial temperature of 50 °C.

Table 1 - Methane/propane and a synthetic natural gas compositions

	C_1/C_3	Synthetic Natural Gas (SNG)
CH_4	92 mol%	82 mol%
C_2H_6	8 mol%	10.5 mol%
C_3H_8	----	6.3 mol%
IC_4	----	1.2 mol%

The aqueous (with or without additive) and oil phases used in the experiments were fed into the rock-flow cell. After sealing the cell, a vacuum pump removed any air dissolved in the liquid phases. The syringe pump was then used to pressurize the cell with the gas until the desired pressure was achieved. The cell was heated to 50 °C (the temperature at which we are outside the wax deposition region). After the oil phase was saturated with gas, the cell was kept still in a horizontal position, simulating the shut-in and avoiding the hydrate formation during the cooling stage.

The cell was cooled down until 4 °C, at a cooling rate of 7 ºC per hour. To simulate the restart, the desired oscillation rate was set, allowing for rapid hydrate formation and the test began to be analyzed and monitored via P, T, V, and visualization. It was assumed that the system reached steady-state and the end of the experiment when changes in the hydrate formation and volume variations in the syringe pump could no longer be measured.

A total of 26 experiments were performed with different filling compositions, pressure, and temperature conditions, as listed in Table 2. Moreover, it was evaluated the effect of subcooling, salt concentration, liquid loading, and water cut in the hydrate formation.

Table 2 – Test matrix

#	Gas phase	NaCl + $CaCl_2$ [wt%]	P (bar)	LL [%]	WC [%]	T_F [°C]	ΔT [°C][(1)]	HFRI (Mid) a|d|b	HFRI (Final) a|d|b	HRFI[(2)]	C [%][(3)]
1	SNG	0	60	30	40	4	15	1|1|0	1|1|1	5	20
2	C_1/C_3	3.3	60	30	10	4	13	1|1c|0	1|1c|0	4	14
3	C_1/C_3	3.3	60	30	30	4	13	1|1c|1	1|2a|1	7	24
4	C_1/C_3	3.3	60	30	50	4	13	2|1c|1	2|2a|2	10	10
5	C_1/C_3	16	60	30	10	4	7	1|0|0	1|1c|0	3	37
6	C_1/C_3	16	60	30	30	4	7	1|1c|1	1|1a|1	6	26
7	C_1/C_3	16	60	30	50	4	7	2|1c|1	2|2a|2	10	14
8	C_1/C_3	0	60	60	10	4	15	1|0|0	1|0|0	2	44
9	SNG	0	60	60	10	4	15	1|0|0	1|0|0	2	42
10	SNG	0	60	60	50	4	15	2|2a|1	2|2a|2	11	9
11	SNG	3.3	60	60	50	2	15	2|1c|1	2|2a|2	10	10
12	SNG	16	60	60	50	-5	15	2|1c|1	2|2a|2	10	19
13	SNG	16	60	60	50	0	10	2|2a|1	2|2a|2	11	28
14	SNG	16	60	60	50	5	5	----	----	----	----
15	SNG	16	80	60	50	-3	15	1|2a|1	2|2a|2	10	10
16	SNG	16	80	60	30	-3	15	1|1c|0	1|1c|0	4	17
17	SNG	16	80	60	30	2	10	1|1c|0	1|1c|0	4	19
18	SNG	16	80	60	30	7	5	1|0|0	1|0|0	4	9
19	SNG	3.3	80	60	30	4	15	1|1c|0	2|1c|0	5	33
20	SNG	0	80	60	30	6	15	1|1c|0	2|1c|0	5	52
21	SNG	16	80	60	40	-3	15	0,5|0|0	0,5|0|0	1	32
22	SNG	16	80	60	40	7	5	0,5|0|0	0,5|0|0	1	18
23	SNG	3.3	80	60	10	2	15	0,5|0|0	0,5|0|0	1	19
24	SNG	3.3	80	60	10	12	5	0,5|1b|0	0,5|0|0	2	16
25	SNG	0	80	60	10	4	15	0,5|0|0	0,5|0|0	1	17
26	SNG	0	80	60	10	14	5	0,5|1b|0	0,5|0|0	2	22
27	SNG	0	80	60	30	6	15	0|0|0	0|0|0	0	44
28	SNG	16	80	60	30	-3	15	3|2a|4	3|2a|4	21	22

29	SNG	0	80	20	30	6	15	3|1|0	0.5|1c|0	4	31
31	SNG	16	80	20	30	7	5	3|0|4	0.5|1|0	19	47

(1) Subcooling; (2) Hydrate flow risk index – total(mid+final); (3) Water conversion.

3. RESULTS AND DISCUSSION

After the formation of hydrates, the system is assessed using an analysis methodology, which consists of feeding an index based on weights attributed to the respective morphologies of formed hydrates. These are based on the possibilities of formation and how dangerous these profiles are, and their combinations for the management of the hydrates (Melchuna et al., 2020). The score, as seen in Figure 3, is based on combinations of aggregation, deposition, and bedding profiles.

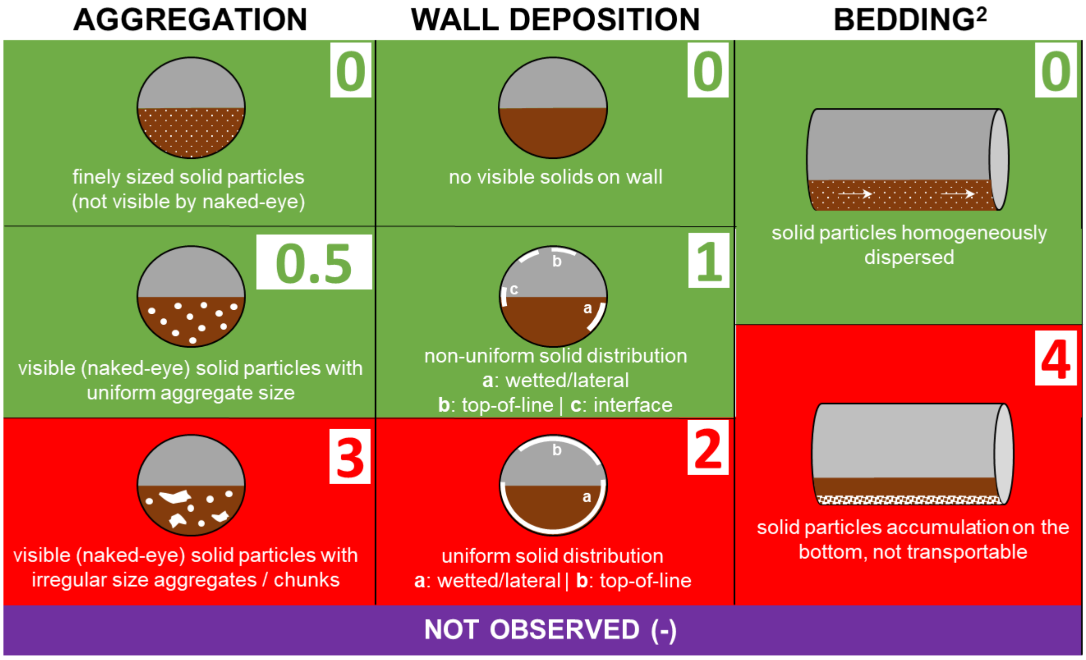

Figure 3 - Hydrate flow risk scoring
Source: Adapted from (Melchuna et al., 2020)

An index is calculated on the combinations and with the detailed views of the intermediate and final stage, we are able to assign a risk value and talk about the reliability of those tests under the conditions. A summary of these observations can be found in Table 2 previously presented.

The experimental data presents a series of tests evaluating the relationship between salt concentration, water cut, subcooling, liquid load, etc. In Test 1, which had 0% salt, the conversion rate reached 50%. However, in Test 2, where the salt concentration increased to 3.3%, the conversion rate dropped significantly to 28%. Further, in Test 3, with a higher salt concentration of 16%, the conversion rate decreased even further to 15%. It can be seen in Figure 3. From these observations, it can be inferred that there is a negative correlation between salt concentration and conversion rate to this data set. As the salt concentration increases, the conversion rate decreases. This suggests that the presence of salt has an inhibitory effect on the conversion process being tested. Furthermore, the data also indicates that the risk associated with higher water content increases when compared to conditions with lower water content.. Water cut refers to the proportion of water in a mixture, and a higher water cut implies a greater risk. The presence of salt seems to decrease this risk, potentially leading to a more dispersed distribution.

According to Figure 4, for a scenario where the other variables, such as subcooling, water cut, pressure, etc. are kept constant, and the salt concentration varies, it is observed that the increase in salt concentration favors the dispersion of hydrates, migrating my system to a safe operational condition, based on scoring from the flow risk.

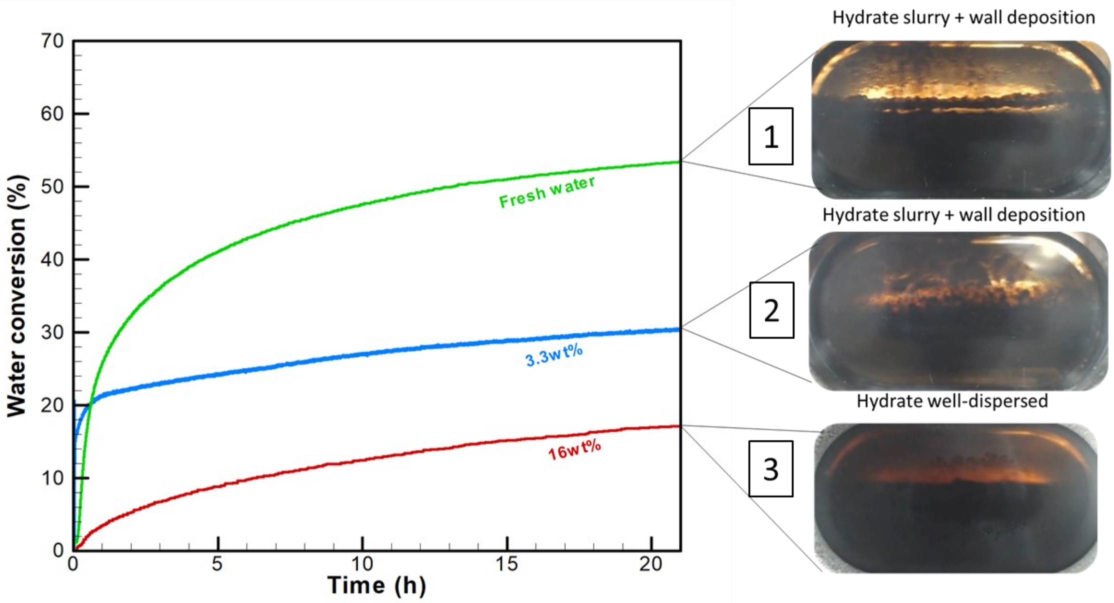

Figure 4 – 1) Hydrate slurry + wall deposition; 2) Hydrate slurry + wall deposition; 3) Hydrate well dispersed; Conditions and contents: SNG / Bacalhau crude oil / 80 bar / 60% LL / 30% WC / ΔT = 15°C / 0, 3.3, 16 wt% salt

Managing hydrate formation in a three-phase system involves employing various strategies. These include maintaining appropriate temperature and pressure conditions to avoid the hydrate stability zone, using thermodynamic hydrate inhibitors, and implementing separation techniques to reduce the water cut before it reaches critical points in the system.

The water cut of a system is a crucial variable of the flow assurance study by the simple relation that a greater amount of available water would imply a high amount of hydrates, when under optimal pressure and temperature conditions. However, not necessarily a large amount of water implies a greater risk, this will be directly dependent on other variables such as subcooling or salt concentration. Higher water cuts mean a greater proportion of water relative to the other phases. The higher the water cut, the more water molecules are available for hydrate formation, resulting in an elevated risk of hydrate blockages or flow assurance issues.

This trend can be seen between Figure 6 to Figure 8 where this risk tends to increase as the points stand out in the region with the highest water cut. Notably, in this risk tends to increase as the points stand out in the region with the highest water cut evaluated: aggregation, deposition, and bedding. in the center of the square (A|D|B), the indexes are represented. In the upper left part, we can visualize the experiment number (1-31), and in the upper right part, we have the liquid load of each test (20 - 60%). At the bottom right, the estimated hydrate conversion is given (%). The colors of the squares represent whether the system has a safe or unsafe condition based on the formed morphology. All this information is summarized in Figure 5, which brings a subtitle representing the visual way of reading the data described in the graphs shown between Figure 6 to Figure 8.

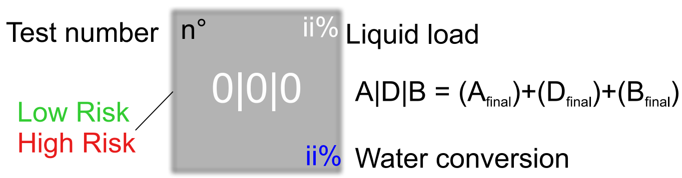

Figure 5 – Content subtitle

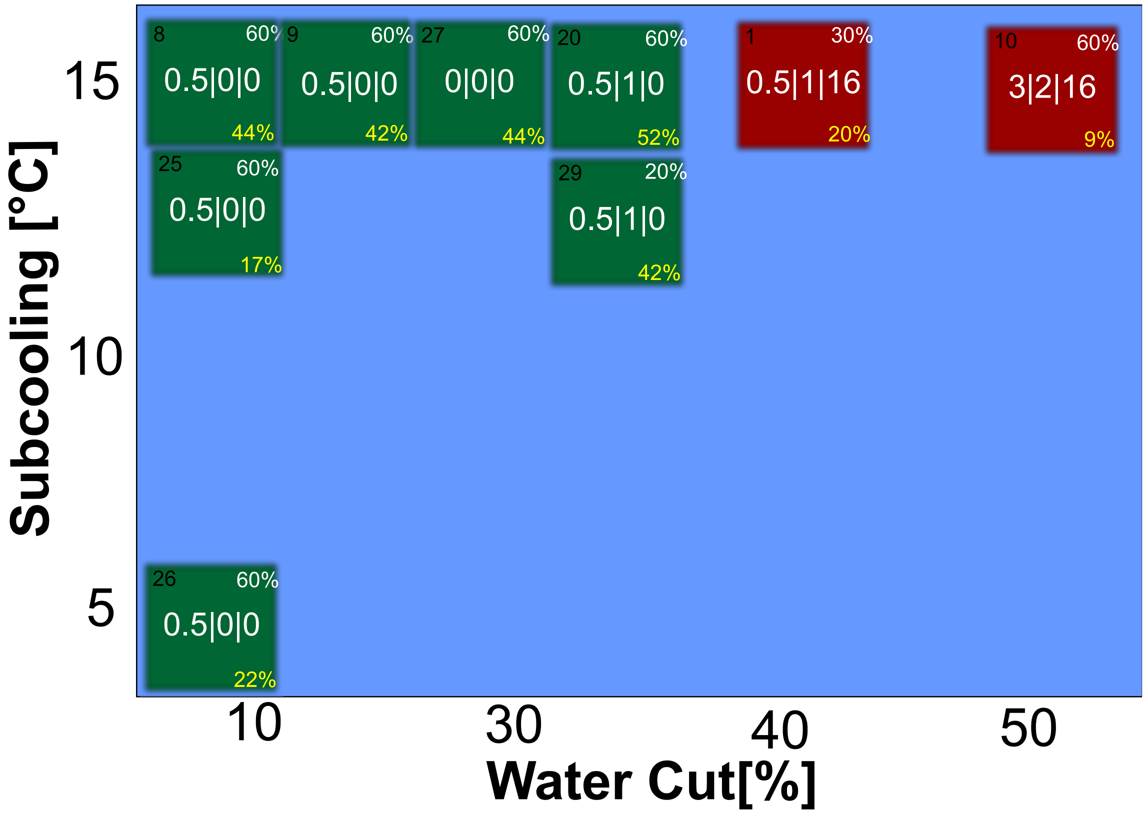

Figure 6 – Summary of the results based on the correlation between subcooling and water cut for the non-inhibited system cut

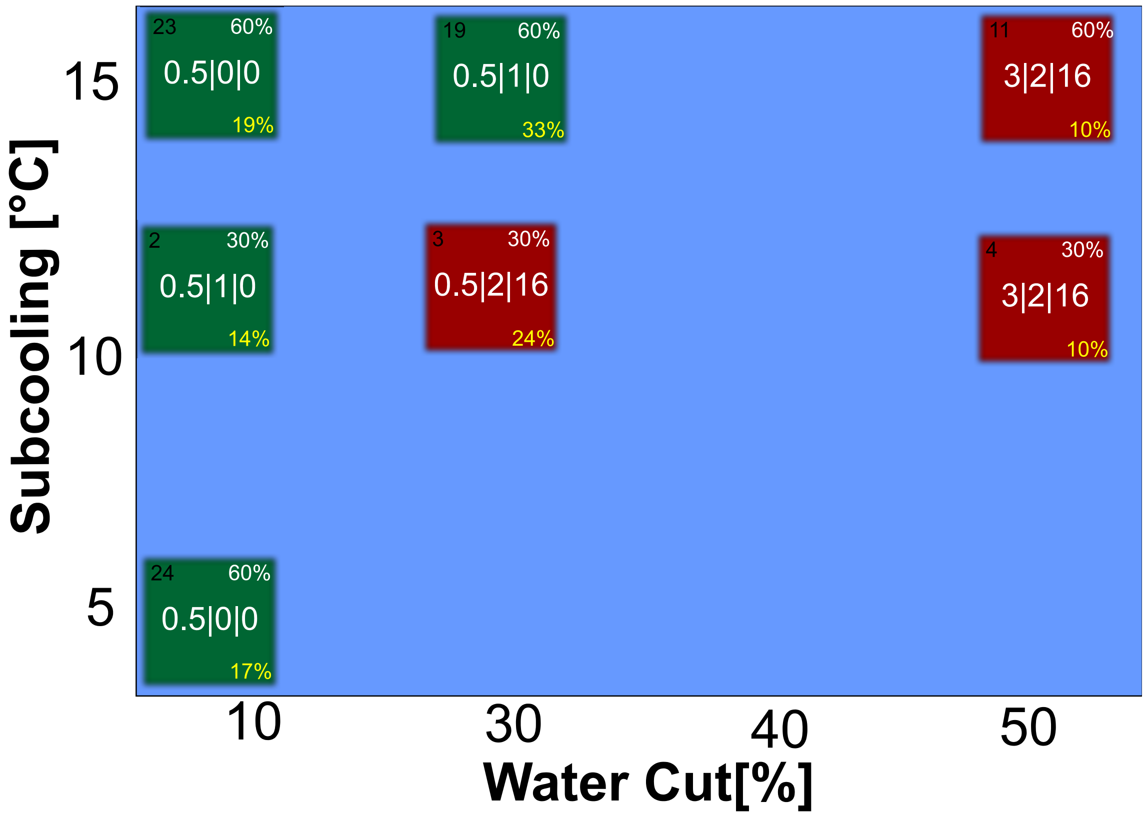

Figure 7 – Summary of the results based on the correlation between subcooling and water cut for the system with 3.3 wt% brine.

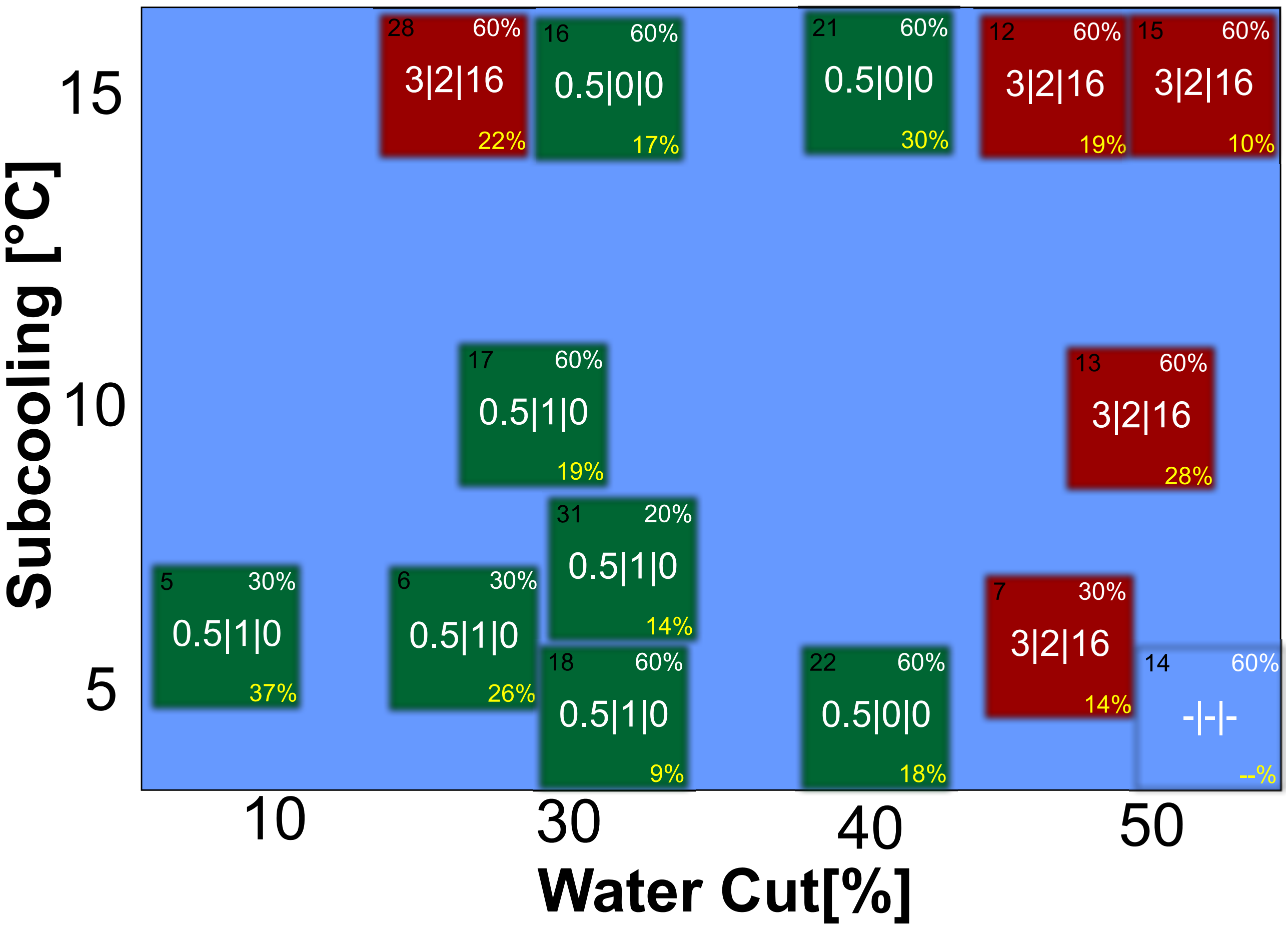

Figure 8 – Summary of the results based on the correlation
between subcooling and water cut for the system with 16 wt% brine.

In addition to the observed correlation wherein higher water content increases the likelihood of the system entering an unsafe condition, Figures 6 to 8 also illustrate a corresponding trend. Specifically, these figures demonstrate that as salt concentration increases, the probability of encountering an unsafe state diminishes. This effect remains consistent even in scenarios characterized by substantial water content. Notably, in the case of test 14, the formation of hydrates was not observed. Consequently, the representation of this test continues without additional data, and a repeat test under identical conditions will be conducted later. Test 30 is still in progress and its implementation was postponed for practical purposes of the test schedule

3.1 Partial conclusions

Proper management and mitigation strategies, considering factors such as subcooling, water cuts, and hydrate inhibitors, are essential for ensuring the safe and efficient operation of oil and gas production systems.

In summary, the following observations were made:

- An increase in salt concentration promoted the dispersion of hydrates.
- The morphology and deposition of hydrates remained unaffected in saline systems.
- With increasing water cut, there was a higher risk of agglomeration and deposition.

4. ACKNOWLEDGEMENTS

To NUEM and Equinor for the partnership and funding of the project.

5. REFERENCES

Inemugha, D. A., Ajienka, J. A., & Student, M. T. (2020). Hydrate Management-Effect of Water Cuts on the Cool Down Times of an Unplanned Shutdown. In *IJESC*. http://ijesc.org/

Liu, Z., Wang, J., Liu, W., Li, Y., Lang, C., Zhang, M., & Song, Y. (2022). Effect of brine salinity on the rheological properties of hydrate-in-oil slurries. *Journal of Petroleum Science and Engineering*, *208*(PE), 109756. https://doi.org/10.1016/j.petrol.2021.109756

Mali, G. A., Chapoy, A., & Tohidi, B. (2018). Investigation into the effect of subcooling on the kinetics of hydrate formation. *Journal of Chemical Thermodynamics*, *117*, 91–96. https://doi.org/10.1016/j.jct.2017.08.014

Melchuna, A., Zhang, X., Sa, J. H., Abadie, E., Glénat, P., & Sum, A. K. (2020). Flow Risk Index: A New Metric for Solid Precipitation Assessment in Flow Assurance Management Applied to Gas Hydrate Transportability. *Energy and Fuels*, *34*(8), 9371–9378. https://doi.org/10.1021/acs.energyfuels.0c01203

Ren, Z., Liu, D., Liu, Z., & Pan, Z. (2020). Influence of sodium chloride on the kinetics of methane hydrate formation in the presence of surfactant. *Journal of Natural Gas Science and Engineering*, *83*(August), 103622. https://doi.org/10.1016/j.jngse.2020.103622

Umuteme, O. M., Zahidul Islam, S., Hossain, M., & Karnik, A. (2022). An improved computational fluid dynamics (CFD) model for predicting hydrate deposition rate and wall shear stress in offshore gas-dominated pipeline. *Journal of Natural Gas Science and Engineering*, *107*. https://doi.org/10.1016/j.jngse.2022.104800

Zerpa, L. E., Salager, J. L., Koh, C. A., Sloan, E. D., & Sum, A. K. (2011). Surface chemistry and gas hydrates in flow assurance. *Industrial and Engineering Chemistry Research*, *50*(1), 188–197. https://doi.org/10.1021/ie100873k

Zhou, S., Chen, X., He, C., Wang, S., Zhao, S., & Lv, X. (2018). Experimental study on hydrate formation and flow characteristics with high water cuts. *Energies*, *11*(10). https://doi.org/10.3390/en11100000

6. RESPONSIBILITY NOTICE

The author(s) is (are) the only responsible for the printed material included in this paper.